JOURNAL OF AIRCRAFT
Vol. 48, No. 4, July–August 2011

Industrial Application of Robust Aeroelastic Analysis

Martin Carlsson Leijonhufvud* and Anders Karlsson†
Saab AB, SE-581 88 Linköping, Sweden

DOI: 10.2514/1.C031170

The recently developed μ-p method for robust aeroelastic analysis is applied to a case study concerning the aeroelastic analysis of a fighter aircraft equipped with a new wingtip missile. A process for using robust analysis for industrial applications is developed and discussed. The process combines robust analysis, flight flutter testing, and model validation in a way suitable for industrial purposes. Aerodynamic uncertainties in terms of pressure variations in the wingtip area are considered. First, a sensitivity analysis is performed to investigate how much effect uncertainties in different areas of the aerodynamic model have on the damping. The results from the sensitivity analysis are used to choose a suitable uncertainty model. Robust aeroelastic analysis is then performed, with the focus on possible damping variations at different flight conditions. Finally, a closely coupled procedure combining flight flutter testing, uncertainty model validation, and robust analysis is applied for successive expansion of the flight envelope and to show that the aircraft is free from aeroelastic instabilities.

I. Introduction

AEROELASTIC analysis and flight flutter testing (FFT) are central and important topics in aircraft airworthiness assessment. Confident results from numerical analysis are necessary in order to obtain an efficient and reliable flutter clearance process. There are, however, numerous sources of model uncertainties involved in aeroelastic analysis. The aerodynamics are often claimed to be the most dominant source, but structural uncertainties in terms of variations in mass and stiffness properties may sometimes also be significant; see Pettit [1]. Considering FFT, this is an expensive activity that could be associated with high risk. Here as well, a systematic and reliable experimental procedure is required to obtain confident experimental data in a safe yet efficient manner. The number of gathered data points from fight testing is usually very limited. This fact often makes robust analysis methods based on statistics less usable in practice.

So-called μ analysis, originating from the control community, provides a framework for robust stability analysis considering deterministic uncertainty [2]. The first initiatives of using μ analysis for aeroelastic applications were performed by Lind and Brenner [3,4]. Additional relevant efforts on combining aeroelasticity and μ analysis can be found in [5–7]. Borglund later combined μ analysis with classical frequency-domain flutter analysis and developed the μ-k method [8]. By applying this method, the standard numerical tools, in terms of FE structural models and panel-type aerodynamics, can be extended to cover robust flutter analysis. Moreover, the method allows for straightforward inclusion of aerodynamic uncertainties, which is a significant advantage for aeroelastic applications [9,10]. However, the μ-k method (and similar formulations) suffers from an important drawback when it comes to industrial applications. The method focuses only on computing the worst-case (or best-case) critical flutter speed for a given set of model uncertainties or variations. The robust stability boundary is an important result but, for practical applications, it is usually also desirable to predict robust aeroelastic properties at subcritical flight conditions. Also, for obvious reasons, FFT is usually not taken to the actual point of flutter instability. Hence, the method suffers from shortcomings when considering the model validation aspects.

Recently, Borglund developed the μ-p method, which is, in essence, a generalization of the μ-k method to cover the Laplace domain [11]. Using this new method, robust analysis can be performed to investigate aeroelastic properties at any flight condition. For example, properties such as possible damping variations due to a given model uncertainty at a certain flight condition can be investigated. Hereby, the method can also be used for sensitivity analysis. The method allows for straightforward comparison between analysis and flight-test data and provides good possibilities for model validation. Early attempts at using the new μ-p method in industry have been made as reported in [12]. The purpose of the current paper is to present a more recent industrial application of robust aeroelastic analysis in the μ-p framework and to show a method for combining robust analysis and FFT that has been developed and evaluated. This paper focuses on a case study considering the flutter clearance process of a new air-to-air missile on the Saab Gripen fighter aircraft.

II. Robust Aeroelastic Analysis

The equations of motion of an aeroelastic system can be expressed according to

$$\boldsymbol{F}_0(p)\boldsymbol{\eta} = [\boldsymbol{M}_0 p^2 + (L^2/u^2)\boldsymbol{K}_0 - (\rho L^2/2)\boldsymbol{Q}_0(p, M)]\boldsymbol{\eta} = \boldsymbol{0} \quad (1)$$

where $\boldsymbol{M}_0$ is the modal mass matrix, $\boldsymbol{K}_0$ is the modal stiffness matrix, $\boldsymbol{Q}_0(p, M)$ is the aerodynamic transfer matrix, sometimes called the generalized aerodynamic force matrix, and $\boldsymbol{\eta}$ is the vector of modal coordinates. The airspeed is denoted u, and L is the reference length. Moreover, ρ is the air density, M is the Mach number, and $p = g + ik$ is the nondimensional Laplace variable, where g represents the real (damping) part of the eigenvalue and k is the reduced frequency.

The flutter equation is a nonlinear eigenvalue problem and can, for each flight condition, be solved for a set of complex eigenvalues $p = g + ik$ with associated eigenvectors $\boldsymbol{\eta}$. It is common practice to solve the flutter equation approximately using, for example, the p-k [13] or g method [14]. At a given altitude, the flutter equation can be solved for increasing airspeed (or Mach number). By using this approach, the stability boundary can be found by detecting the flight condition where some eigenvalue reaches the stability boundary at $g = 0$. At this flight condition, there is a critical eigenvalue $p = ik$ making the transfer matrix $\boldsymbol{F}_0(p)$ singular. This approach for aeroelastic analysis can be viewed upon as the standard procedure and, in the following, is referred to as nominal analysis.

Now, consider parametric uncertainties in the system matrices that can be represented by unknown but bounded parameters in the vector $\boldsymbol{\delta}$. The aeroelastic equation (1) can then be expressed as

Received 6 July 2010; revision received 18 January 2011; accepted for publication 17 February 2011.

*Senior Aeronautical Engineer, Saab Aerosystems, Br. Ugglas Gata. Member AIAA.

†Technology Leader, Saab Aerosystems, Br. Ugglas Gata. Member AIAA.

$$[\boldsymbol{M}(\boldsymbol{\delta})p^2 + (L^2/u^2)\boldsymbol{K}(\boldsymbol{\delta}) - (\rho L^2/2)\boldsymbol{Q}(p, M, \boldsymbol{\delta})]\boldsymbol{\eta} = \boldsymbol{0} \quad (2)$$

The uncertainty parameters can be both real and complex, typically representing structural and aerodynamic uncertainties, respectively. It is also assumed that the uncertainty parameters have been scaled, such that $|\delta_j| \leq 1$ holds for each parameter, and that $\delta = \boldsymbol{0}$ gives the nominal matrices according to

$$\boldsymbol{M}(0) = \boldsymbol{M}_0, \qquad \boldsymbol{K}(0) = \boldsymbol{K}_0, \qquad \boldsymbol{Q}(p, M, 0) = \boldsymbol{Q}_0(p, M) \quad (3)$$

This means that each $\boldsymbol{\delta}$ belongs to set D, defined as $D = \{\boldsymbol{\delta} : \|\boldsymbol{\delta}\|_\infty \leq 1\}$. Equation (2) is an uncertain nonlinear eigenvalue problem that, for each choice of the parameters $\boldsymbol{\delta}$, defines a set of eigenvalues p and corresponding eigenvectors $\boldsymbol{\eta}$. In very simple cases, it may be possible to compute the regions of all possible eigenvalues for a certain parametric variation $\boldsymbol{\delta} \in D$ by performing a systematic search in the parameter space. This approach, however, soon becomes practically infeasible when the number of uncertain parameters increases.

A. μ-p Method for Robust Aeroelastic Analysis

Very briefly, the μ-p flutter method uses μ analysis to determine if a certain eigenvalue p is a feasible solution to the uncertain flutter equation (2) for some parameters $\boldsymbol{\delta} \in D$ [11]. By using line-search types of algorithms, the regions of feasible eigenvalues in the complex plane can be efficiently computed. Of particular concern are the eigenvalues p_- and p_+ within the feasible regions of each aeroelastic mode having the minimum and maximum real parts, respectively. These eigenvalues provide damping bounds for the aeroelastic mode. If p_+ has a negative real part for all aeroelastic modes at a certain flight condition, the aircraft is said to be robustly stable.

B. Model Validation in μ-p Framework

Choosing the structure of the uncertainty model is a matter of parameter selection. This can usually be done based on physical reasoning and engineering insight. Estimating the uncertainty magnitudes (bounds) of the parameters may, however, be more of a concern. Too low uncertainty magnitudes will not capture the worst-case perturbation, whereas too high magnitude will give excessively conservative results. Fortunately, the μ-p framework offers straightforward possibilities for matching the uncertainty magnitudes based on experimental data. By using so-called p validation [11], experimental data in terms of a measured eigenvalue $p_{\text{exp}} = g_{\text{exp}} + ik_{\text{exp}}$ (i.e., damping and frequency of a certain aeroelastic mode) at some tested flight conditions can directly be used to adjust the uncertainty magnitudes. Given the uncertainty model structure (parameters), μ analysis is used to compute the minimum uncertainty magnitude (in terms of the norm of the uncertainty matrix) $\bar{\sigma}_p$ that expands the computed eigenvalue set such that the measured eigenvalue is included. For example, a $\bar{\sigma}_p$ value of 0.5 would here mean that only 50% of the initially assumed uncertainty magnitudes are required to include the experimental eigenvalue. The uncertainty magnitudes can therefore, in this case, be scaled by 0.5. More details about how $\bar{\sigma}_p$ is calculated and the relation to the values of the uncertainty parameters are given in [11].

Sometimes, it can be more efficient to only consider the measured damping of an aeroelastic mode when performing the validation. This approach is referred to as g validation [11]. The minimum uncertainty magnitude (in this case, denoted $\bar{\sigma}_g$) required to make an eigenvalue have the real part $g = g_{\text{exp}}$ is computed here. This method is particularly beneficial if the applied uncertainty model cannot capture offsets in frequency very well. Using experimentally measured frequencies for validation would, in such a case, lead to very conservative results in terms of large damping variations. In this work, g validation is applied for model validation; see Sec. IV.E.

C. Aerodynamic Uncertainty Modeling

Only aerodynamic uncertainty is treated in this study although, it is also possible to consider uncertainties in the structural model [15,16]. A standard panel-type aerodynamic model is used in this study; see Sec. III.B. Each aerodynamic panel (lifting surface) is divided into aerodynamic elements (sometimes called aerodynamic boxes). It is, for this investigation, desirable to apply aerodynamic uncertainty parameters associated with specific areas (i.e., elements) of the aerodynamic model. This is not possible by applying parameters directly on the aerodynamic matrix $\boldsymbol{Q}_0$ in modal form. However, the computable nominal aerodynamic transfer matrix $\boldsymbol{Q}_0(k, M)$ can be partitioned in one left partition and one right partition according to

$$\boldsymbol{Q}_0(k, M) = \boldsymbol{L}\boldsymbol{R}(k, M) \quad (4)$$

where the matrix $\boldsymbol{L}$ contains information about the structural modes and the coupling between the structural and aerodynamic models. Hence, $\boldsymbol{L}$ is constant and defines the mapping from pressure coefficients on the individual aerodynamic elements to modal forces. The right matrix $\boldsymbol{R}(k, M)$ defines the mapping from modal coordinates to aerodynamic surface pressure coefficients. The in-house program AEREL, used at Saab for unsteady aerodynamic calculations, gives the $\boldsymbol{L}$ and $\boldsymbol{R}(k, M)$ matrices as output during the analysis [17,18]. It is also possible to get these matrices from other programs, such as NASTRAN and ZAERO, as reported in [9]. By doing this partitioning of the nominal $\boldsymbol{Q}_0$ matrix, it is possible to assign different uncertainty parameters to the individual lifting surface pressure coefficients of the aerodynamic model according to

$$c_p = (1 + w_j\delta_j)c_{p0} \quad (5)$$

where c_{p0} is the nominal complex pressure coefficient and δ_j is the complex uncertainty parameter, which is scaled such that $|\delta_j| \leq 1$. Typically, the elements of the aerodynamic model are grouped into patches, with individual real weights w_j setting the level of uncertainty at different areas of the aerodynamic model. A weight $w_j = 0.1$ for a certain patch of elements corresponds, here, to 10% uncertainty in the (complex) pressure coefficient for all elements within that patch. The pressure coefficients within each patch are assumed to be perturbed in a uniform manner. This approach enables a physical representation of the aerodynamic uncertainties, since the uncertainties can be applied to certain areas of the aerodynamic model. For a more thorough description of the construction of aerodynamic uncertainties, see [9].

III. Case Study Configuration

This study is a part of the integration and flutter clearance processes of a new external store on the Swedish Saab Gripen fighter aircraft. The store that is integrated is the European infrared imaging system–tail/thrust vector-controlled (IRIS-T) air-to-air missile. Figure 1 shows the Gripen demonstrator (Demo) aircraft (dual seat) with IRIS-T in the wingtips. The aeroelastic clearance process involves flutter analysis of a substantial number of store configurations and FFT of some selected configurations. This study focuses on a Gripen C (single seat) air-to-air fighter configuration with two

Fig. 1 Gripen Demo with two IRIS-T missiles in wingtip (Copyright Gripen International. Photographer: Katsuhiko Tokunaga).

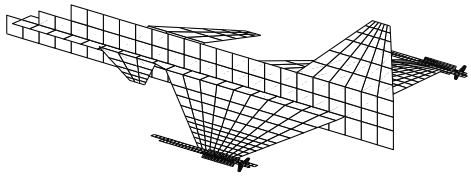

Fig. 2 Aerodynamic model of Gripen C, including two IRIS-T missiles at the wingtips.

IRIS-T missiles mounted in the left and right wingtips. For conciseness, only results for flight conditions at 1 km altitude are shown and discussed within this paper. Quantitatively authentic results from analysis and flight tests are presented. For reasons of confidentiality, the results are, however, presented without stating the exact aircraft configuration, numerical values, and flight conditions. The general results and conclusions from the investigation are, however, not affected by these actions.

A. Structural Models

A standard-type linear FE model, developed in ASKA software (Saab in-house), is used as a structural model for the analysis. The structural FE model of the clean aircraft had previously been extensively validated and calibrated in several ground vibration tests (GVTs). The new missile is modeled as an elastic beam with representative stiffness and mass distributions. The attachment between the missile and the wingtip is modeled using connecting spring elements with correct stiffness properties. A GVT was performed for the complete aircraft, including the new wingtip missiles. Only small deviations were observed when comparing the modal data from FE analysis and GVT. Uncertainty associated with the structural model is hence considered to be small, and it is therefore not accounted for in this investigation. From the FE model, the structural mode shapes with associated modal mass and natural frequencies are extracted. For reasons of efficiency, the modal basis in this study is confined to 10 structural modes. Analyses using 30 structural modes have also been performed, but it was concluded that the additional modes did not significantly affect the results presented in this paper.

B. Aerodynamic Model

The AEREL program is used to compute the unsteady aerodynamic forces. The panel model of Gripen C, including two IRIS-T missiles, is shown in Fig. 2. The panel model is coupled to the structural model using interpolation with polynomial functions, and the nominal aerodynamic transfer matrices $\boldsymbol{Q}_0(k, M)$ are computed. The nominal aerodynamic models of the aircraft and missile have previously been validated against steady wind-tunnel data, showing good agreement. The aerodynamics of the missile, which is of particular interest in this study, was investigated, not only for the free-flying missile, but also when mounted on the aircraft: i.e., including the interference aerodynamics from the aircraft. Although the aerodynamic model has been validated with good results with respect to steady aerodynamics (i.e., for $k = 0$), there could still be uncertainties associated with the new missile aerodynamics, especially when considering the unsteady effects ($k \neq 0$).

IV. Process for Robust Aeroelastic Analysis and Flight Flutter Testing

The process for the robust aeroelastic analysis and FFT developed within this work is shown in Fig. 3. In short, the process starts with classical flutter analysis (referred to as nominal analysis), and it continues with sensitivity analysis, uncertainty modeling, and preflight robust analysis. The final step in the airworthiness assessment is a closely coupled successive FFT/analysis approach, where the uncertainty model is continuously updated based on the outcome from the FFT. Each step of the analysis process is further described in the following sections.

A. Nominal Analysis

As a first step in the airworthiness assessment, a nominal flutter analysis is performed. No structural damping is, in this case, included in the analysis; therefore, the results may be treated as somewhat conservative with respect to the damping level. Figure 4 shows the damping and frequency for the four dominating aeroelastic modes. The Mach number is, in this paper, presented as a relative Mach number: i.e., the actual Mach number divided by the envelope limit Mach number. Hence, a $M/M_{\max}$ value of 1.0 corresponds to the speed envelope limit at the current altitude. Note that positive damping here corresponds to a stable condition; that is, the real part of the eigenvalue is negative. As shown, no instability is predicted within the flight envelope. The aeroelastic mode numbers 3 and 4 are found to be the most critical, showing the lowest damping with a decreasing trend toward the envelope limit. Therefore, the following results and discussion focus on these two aeroelastic modes. Aeroelastic mode number 3 is dominated by symmetric wingtip torsion, whereas aeroelastic mode number 4 is dominated by antisymmetric wingtip torsion.

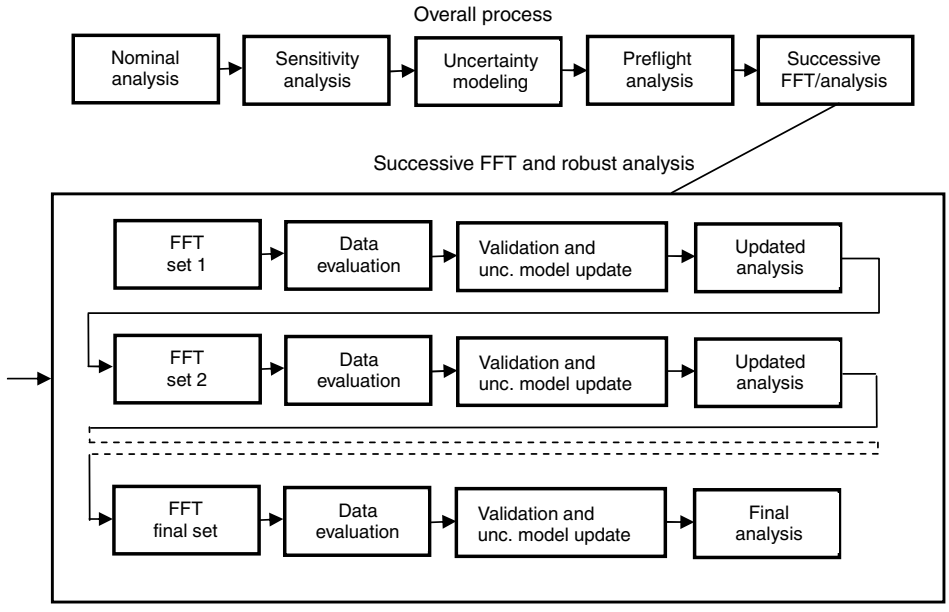

Fig. 3 Flowchart of combined analysis and FFT process (unc. denotes uncertainty).

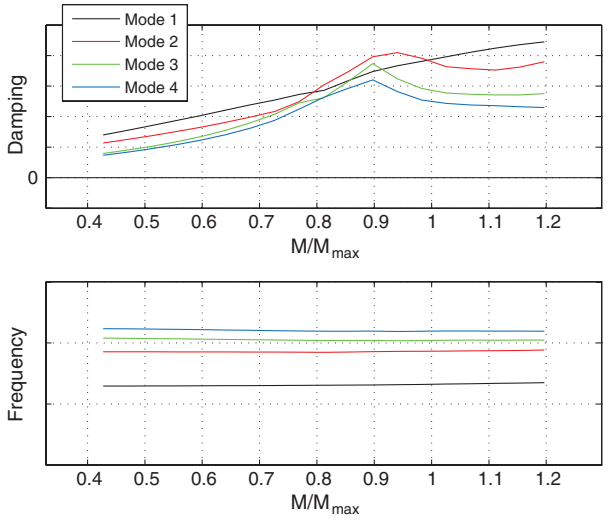

Fig. 4 Frequency and damping versus Mach number for the first four aeroelastic modes.

B. Sensitivity Analysis

Before choosing the actual uncertainty description to be applied, it is useful to perform a sensitivity analysis focusing on the most interesting aeroelastic modes. By using g validation, as described in Sec. II.B, it is possible to estimate how much influence different uncertainty parameters have on the damping of each mode of interest. Here, an uncertainty model where each uncertainty patch corresponds to an individual aerodynamic element in the area of interest is used for this purpose. The nominal eigenvalue at a certain flight condition is perturbed by adding a small amount of damping (i.e., real part). The uncertainty magnitude $\bar{\sigma}_g$ required to make the eigenvalue with the perturbed real part feasible is then computed for each individual uncertainty patch (here, aerodynamic element). Estimates of damping sensitivities with respect to the various uncertainty parameters can hereby be obtained.

The result from a sensitivity analysis performed within the current study is shown in Fig. 5. The aeroelastic mode number 3 (dominated by symmetric wingtip torsion) is here considered at Mach 0.8 at a 1 km altitude. An uncertainty model containing 612 patches corresponding to the individual aerodynamic elements in the wingtip region (left and right) is applied. The nominal eigenvalue p at the current flight condition is perturbed by adding a small real number. In this specific case, an addition of $(0.001 + 0.0i)$ was used and the minimum magnitude $\bar{\sigma}_{g,j}$ required to make the perturbed eigenvalue feasible was computed for each individual patch (element) j. The required uncertainty norm $\bar{\sigma}_{g,j}$ for each element is, here, directly proportional to the individual uncertainty weight w_j associated with that element. Hence, $\bar{\sigma}_{g,j}$ can be used as a (relative) estimate of the sensitivity $\mathrm{d}(w_j)/\mathrm{d}[\mathrm{real}(p)]$. A small value of $\bar{\sigma}_{g,j}$ means that a small uncertainty magnitude is required to make an eigenvalue with the perturbed damping feasible. For sensitivity illustration, it is therefore more intuitive to use the value $1/\bar{\sigma}_{g,j}$ when plotting the values (corresponding to sensitivity $\mathrm{d}[\mathrm{real}(p)]/\mathrm{d}(w_j)$). Small aerodynamic elements have a relatively small influence on the results. Therefore, the minimum magnitude for each element is also scaled by the area of the actual element in order to illustrate how much influence relative pressure variations in different regions have on the damping of the aeroelastic mode. The value $(1/\bar{\sigma}_{g,j})/a_j$, where a_j is the element area, is used to color the surfaces of the individual elements. As shown, pressure variations in the very tip of the missile and pylon, and in the rear fin region, have a large influence on the damping of the mode, whereas regions in the middle of the missile and the pylon have a much smaller influence. This is natural, since the node line for the dominating structural mode is located approximately in the midchord of the pylon and missile.

C. Uncertainty Modeling

When doing robust aeroelastic analysis, it is, for efficiency reasons, usually practical to use an uncertainty model with relatively few uncertainty patches. Previous investigations have shown that relatively simple uncertainty models with few parameters give fairly similar results to more detailed uncertainty models with a large number of patches as long as the models capture the physical mechanism of interest [12,19]. For this investigation, the choice of uncertainty model structure (i.e., selection of aerodynamic patches) is partly based on the results from the sensitivity analysis described previously. Experience from earlier investigations is, however, also considered. The wingtip region is, here, divided into 17 individual uncertainty patches, as shown in Fig. 6. The aircraft wingtip is divided into three patches, and the pylon and missile body are split into four chordwise patches. Moreover, the four missile guide vanes and four fins are all separate patches.

When robust analysis is to be performed before the flight testing and model validation procedure, the magnitude of the model uncertainties must be set based on experience and engineering judgment. In this case. the magnitude w_j for each uncertainty patch was initially set to 0.10, meaning 10% relative pressure variation. This value was primarily based on experience from validation during earlier investigations involving aerodynamic uncertainty. However, robust analysis with different uncertainty magnitudes can easily be performed, as discussed in the next section. It is possible to apply different magnitudes to the individual patches. In this study, however, the same uncertainty magnitude is used for all patches. The structure of the uncertainty model (selection of patches) is, in this study, the same for all aeroelastic modes and flight conditions, whereas the uncertainty magnitude after validation may vary between modes and flight conditions (as further described in Sec. IV.E).

D. Preflight Robust Analysis

The applied uncertainty model is used to perform robust aeroelastic analysis before the first FFT. Although it is possible to study both frequency and damping variations, the focus during this study is only on possible damping variations at different flight conditions. Since the uncertainty magnitude so far is primarily based on experience from previous investigations, it can be useful to study how much influence the magnitude has on the damping variations. Results from this analysis are shown in Fig. 7, where the upper and

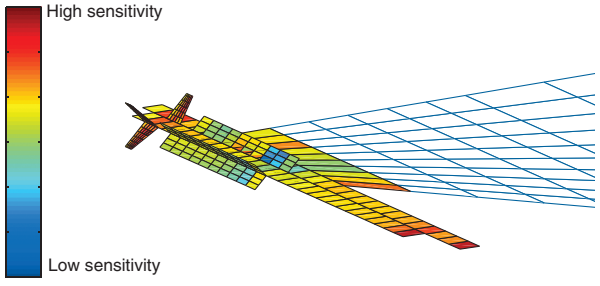

Fig. 5 Damping sensitivity of mode 3 with respect to uncertainty applied to individual aerodynamic elements.

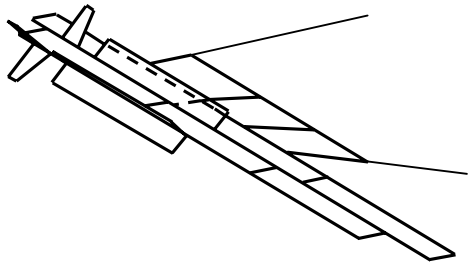

Fig. 6 Illustration of uncertainty model with 17 patches in wingtip area.

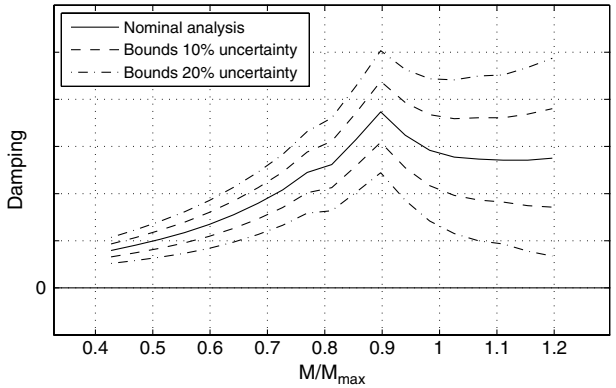

Fig. 7 Robust damping bounds versus Mach number for aeroelastic mode number 3.

lower damping bounds for aeroelastic mode number 3 are plotted for uncertainty magnitudes of 10 and 20% (i.e., using $w_j = 0.1$ and $w_j = 0.2$, respectively). Note that the damping bounds here refer to the damping of the extreme eigenvalues p_- and p_+, with minimum and maximum real parts, respectively [11]. At low speeds, the uncertainties have a relatively small influence on the damping level, whereas the possible damping variations are much higher at high speed. This is natural, since the uncertainties here represent relative pressure variations, and the dynamic pressure is significantly higher at high Mach numbers (constant altitude). In this case, the damping bounds for both uncertainty levels show no risk that the uncertainties can cause instability within the current flight envelope. Here, this holds for all aeroelastic modes, and the aircraft is hence robustly stable with respect to the applied uncertainty models. These types of results are valuable information when planning for FFT. If, for example, the analysis shows that the applied model uncertainties can cause instability in some region of the flight envelope, it may be favorable to be more cautious when performing testing in this region (e.g., use smaller steps when increasing the speed).

E. Flight Flutter Testing

FFT is the ultimate step to show that the aircraft configuration is free from aeroelastic instabilities within the flight envelope. A Gripen test aircraft is used for this purpose. The aircraft is equipped with accelerometers mounted inside the pylons, the fin, the canard, and the fuselage. The positions of the accelerometers are chosen to enable spatial resolution of the aeroelastic modes of interest for the investigation. Excitation is performed using sinusoidal oscillations of the control surfaces, generated by certain flight-test functions implemented in the flight control system. The frequency interval for the excitation is chosen to cover the interesting aeroelastic modes for the particular investigation and store configuration. At each tested flight condition, the aircraft is subjected to different combinations of both symmetrical and antisymmetrical control surface excitations. The measured signals are processed and evaluated using methods for experimental modal analysis. Estimates of the damping, frequency, and mode shape for the most dominant aeroelastic modes are hereby obtained. Each identified aeroelastic mode is characterized by its shape and frequency and compared with the corresponding mode obtained from flutter analysis. Typically, the FFT is started at a high altitude, increasing the airspeed successively until the maximum Mach number is reached. The testing then continues at medium altitude and, finally, the aircraft is tested at low altitude (here 1 km) for increasing speed until the maximum Mach number (or dynamic pressure) is reached.

The FFT and evaluation process is, in addition to the analysis, associated with a significant amount of uncertainties. There are uncertainties considering the accuracy of the tested flight condition (altitude, airspeed, Mach number, etc.), the excitation and measurement (amplification, sampling, filtering, etc.), and the evaluation process (method, frequency windowing, etc.). The noise levels in the measured signals are relatively high (compared with GVT), and repeatability in measurements is often a concern. Typically, the evaluated damping level of an aeroelastic mode may vary significantly between measurements representing the same flight condition, whereas the frequency variations usually are relatively small; see Figs. 8 and 9.

The damping levels from FFT are usually found to be somewhat higher than the numerical predictions. This may partly be due to the

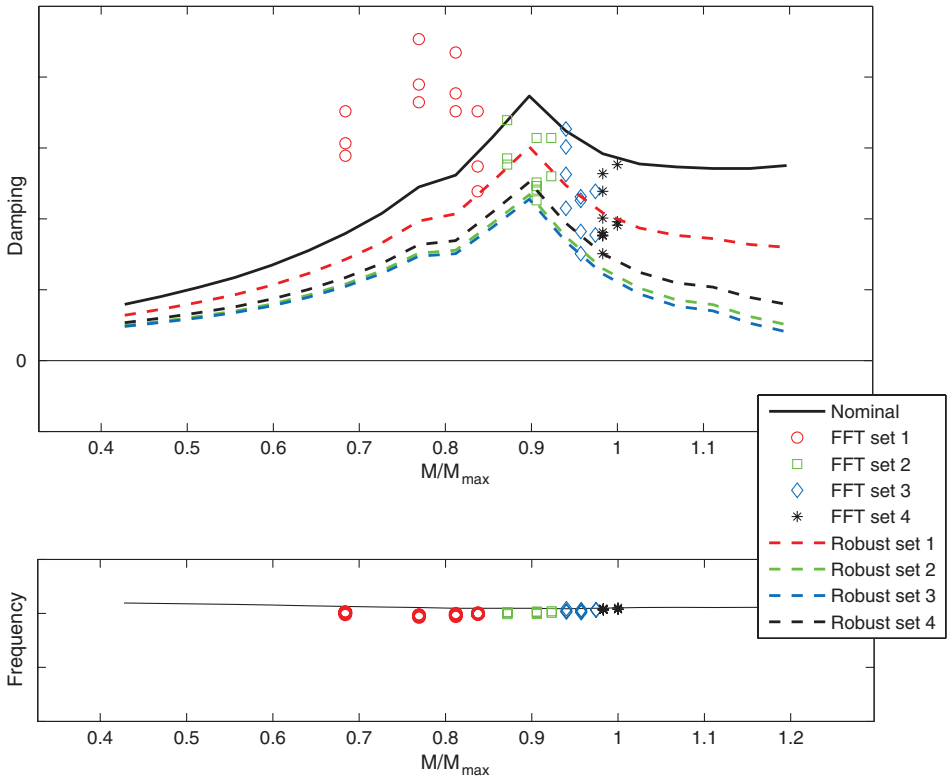

Fig. 8 Results from coupled FFT and robust analysis of aeroelastic mode number 3.

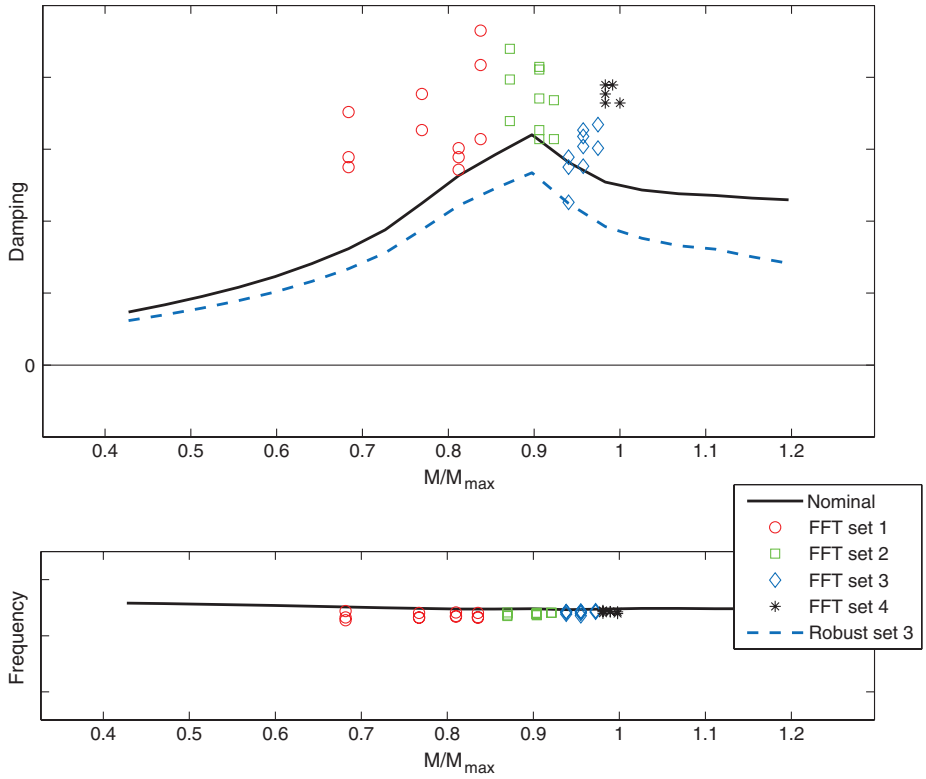

Fig. 9 Results from coupled FFT and robust analysis of aeroelastic mode number 4.

inherent conservative nature of linear aerodynamics and the fact that no structural damping is included in the analysis. There are, however, exceptions and, for some configurations, significant deviations between analysis and experiments are observed. The transonic effects are known to cause reduction in damping, but discrepancies between analysis and flight-test data are sometimes also observed at other flight conditions. During testing, when discovering significant deviations between the FFT results and the numerical predictions, it is desirable to have a well established and confident strategy for making decisions about the continued testing.

A successive FFT process coupled with robust analysis is developed and applied in this study, as shown in Fig. 3. At each altitude where FFT is to be performed, the testing is divided into a number of FFT sets. Each set may include a number of flight conditions, and the Mach number is gradually increased between each set. After completion of each FFT set, the measured data are evaluated and the damping and frequency estimates of each aeroelastic mode of interest are compared with analysis. If some of the damping values show less damping than the nominal prediction, a g validation is performed using the most deviating damping value within the set and the minimum uncertainty magnitude is computed. The uncertainty model is then updated with the new uncertainty magnitude, and a new robust analysis is performed using the updated model. The result from this analysis is then used to decide if it is safe to continue with the next FFT set as planned or if the next set has to be modified with respect to the flight conditions to be tested (i.e., use smaller steps when increasing the Mach number). The validation procedure is applied independently for all aeroelastic modes of interest.

Relatively extensive FFT was performed during this investigation, and testing at some of the flight conditions was repeated in order to gain experience about repeatability issues. The measured signals were evaluated using different methods for experimental modal analysis. Both frequency-domain [20] and time-domain methods [21] were applied. Some modes could also be identified using different types of excitations. Therefore, a number of estimations of the damping and frequency of each aeroelastic mode were available for most of the flight conditions.

The result from the coupled FFT and robust analysis process for mode number 3 is shown in Fig. 8. The FFT at a 1 km (constant) altitude was, here, divided into four sets according to Table 1. The minimum uncertainty magnitudes obtained from validation during each FFT set are summarized in Table 1, and the results from each set are commented on in the following.

For FFT set 1, FFT was performed at four flight conditions with increasing Mach numbers. Most damping values from this first set were found to be higher than the nominal prediction. However, two damping values at the highest Mach number within set 1 were found to be somewhat below the nominal curve. A g validation was therefore performed, and the minimum required uncertainty magnitude was calculated to be 0.11. The uncertainty model was updated, with the uncertainty magnitude set to 0.11 (i.e., using $w_j = 0.11$), and the lower damping bound was calculated (labeled "Robust set 1" in Fig. 8). This updated analysis showed that the aircraft was robustly stable for the flight-test envelope of set number 2, and the testing was continued with the next set of FFT as planned.

For FFT set 2, three flight conditions were tested, and a number of damping values were found to be significantly below the prediction. A new g validation and associated uncertainty model update were hence performed. The updated analysis resulted in a new and significantly lower robust damping bound (labeled "Robust set 2" in

Table 1 Relative Mach numbers and minimum uncertainty magnitudes for each set of FFT

FFT set no.	Tested Mach numbers [M/M max]	Min. uncertainty magnitude, $\bar{\sigma}_g$ mode 3	Min. uncertainty magnitude, $\bar{\sigma}_g$ mode 4
1	0.68, 0.77, 0.81, 0.84	0.11	——
2	0.87, 0.91, 0.92	0.22	——
3	0.94, 0.96, 0.97	0.23	0.089
4	0.98, 1.00	0.19	——

Fig. 8). Still, the analysis showed robust stability for the flight envelope of set number 3, and the testing was continued with the next set of flights.

For FFT set 3, again, damping values significantly below the nominal prediction were observed. Note, however, that the updated robust bound from set 2 essentially captured all the deviations of the measured points in set 3. Only a very small adjustment of the uncertainty magnitude (from 0.22 to 0.23) had to be performed within this step to capture all values. Updated robust analysis was then performed using the updated model. No risk for instabilities was, however, discovered, and the testing could continue with FFT set number 4.

For FFT set 4, after reaching the maximum speed (here, envelope limit) at the current altitude, the damping values from the last FFT set were used to make a final validation, uncertainty model update, and analysis. The results from the final robust analysis were then used to calculate speed margins for robust stability. In this case, no risk for flutter instability was detected within 1.2 times the maximum Mach number.

The corresponding result for aeroelastic mode number 4 is shown in Fig. 9. For this mode, most damping values were found to be significantly higher than predicted by analysis. One damping value from FFT set number 3 was, however, somewhat below the nominal prediction; therefore, a g validation and updated robust analysis were performed after this set. The robust analysis showed no risk for instability for the flight envelope of set 4, and the testing was continued as planned. During the final set, all damping values were found to be higher than the prediction; therefore, no additional robust analyses were performed for this mode.

Note that, for robustness, all damping values obtained from repeated test conditions and evaluations using different methods are considered within each FFT set. An alternative would be to use the mean, or median, damping value at each flight condition. By using all values, the uncertainties associated with the testing and evaluation are, in some sense, accounted for when doing the validation. However, only values that are below the nominal prediction (i.e., where the analysis is nonconservative) are used for updating the uncertainty model. Using the most deviating value, including values significantly above the nominal prediction, would result in excessively conservative results. Also note that the uncertainty magnitude can be both increased and decreased between each FFT set in order to limit the conservativeness of the robust bounds. This coupled FFT and validation approach gives a table (similar to Table 1) with uncertainty magnitudes that are valid for different modes and flight conditions. It is hereby also possible to perform robust analysis using uncertainty magnitudes that vary between flight conditions and modes (i.e., Mach number and frequency-dependent uncertainties). This approach would further limit the conservativeness of the robust analysis.

So far, this new approach for envelope expansion using robust analysis and model validation has not been used as a true online tool using data telemetry during flight testing. Such an implementation of the developed methodology would, however, be possible. Other methods for performing flutter testing using robust analysis exist, such as the flutterometer developed by Lind and Brenner [6]. The flutterometer approach combines μ analysis with a state-space representation of the aeroelastic aircraft to compute robust stability margins. The approach proposed in this study is based on the new μ-p method and applies a standard frequency-domain aeroelastic representation of the aircraft and may, therefore, be considered as closer to classical flutter analysis.

V. Conclusions

This investigation showed that the new μ-p method has great potential to be used in the industrial process for aeroelastic airworthiness assessment. When performing robust aeroelastic analysis, it is important that the applied uncertainty model is representative and can capture the important physical mechanisms of interest for the investigation. In this study, the possibility of applying the μ-p method for sensitivity analysis was found to be very useful when choosing the uncertainty parameters. By using this approach, the number of uncertainty parameters could be limited, and the analysis could be performed efficiently. When it comes to FFT and model validation, it was concluded that care must be taken to limit the conservativeness of the robust analysis. Too extensive conservativeness would otherwise limit the usefulness of the method. The developed process using stepwise FFT and g validation was found to be a useful method for envelope expansion, since it reduced the level of conservativeness. The particular approach outlined in this paper should, however, only be viewed upon as an example of an industrial application of robust analysis. The μ-p method enables a large variety of interesting aeronautical applications.

Acknowledgments

Some of the work within this study was part of the project called "Robust Aeroservoelastic Analysis and Optimization" (NFFP4-S4303) that was financially supported by the Swedish National Program for Aeronautics Research (NFFP). This investigation also serves as a preliminary study within a new research project in the NFFP framework, focusing on the use of robust analysis in the process of airworthiness assessment. The authors express their appreciation to the Flight Dynamics research group at the Royal Institute of Technology (KTH) for excellent support and cooperation. Also, the authors wish to thank Niklas Alskog, Bo Nilsson, and Bengt Winzell at Saab for valuable feedback during the investigation.

References

[1] Pettit, C., "Uncertainty Quantification in Aeroelasticity: Recent Results and Research Challenges," *Journal of Aircraft*, Vol. 41, No. 5, 2004, pp. 1217–1229. doi:10.2514/1.3961

[2] Zhou, K., Doyle, J. C., and Glover, K., *Robust and Optimal Control*, Prentice–Hall, Upper Saddle River, NJ, 1996, Chap. 11.

[3] Lind, R., and Brenner, M., *Robust Aeroservoelastic Stability Analysis*, Springer–Verlag, London, 1999.

[4] Lind, R., "Match-Point Solutions for Robust Flutter Analysis," *Journal of Aircraft*, Vol. 39, No. 1, 2002, pp. 91–99. doi:10.2514/2.2900

[5] Kumar, A., and Balas, G. J., "An Approach to Model Validation in the μ Framework," *Proceedings of the American Control Conference*, Baltimore, MD, IEEE Publ., Piscataway, NJ, 1994, pp. 3021–3026.

[6] Lind, R., and Brenner, M., "Flutterometer: An On-Line Tool to Predict Robust Flutter Margins," *Journal of Aircraft*, Vol. 37, No. 6, 2000, pp. 1105–1112. doi:10.2514/2.2719

[7] Brenner, M., "Aeroservoelastic Model Uncertainty Bound Estimation from Flight Data," *Journal of Guidance, Control, and Dynamics*, Vol. 25, No. 4, 2002, pp. 748–754. doi:10.2514/2.4942

[8] Borglund, D., "The μ-k Method for Robust Flutter Solutions," *Journal of Aircraft*, Vol. 41, No. 5, 2004, pp. 1209–1216. doi:10.2514/1.3062

[9] Borglund, D., and Ringertz, U., "Efficient Computation of Robust Flutter Boundaries Using the μ-k Method," *Journal of Aircraft*, Vol. 43, No. 6, 2006, pp. 1763–1769. doi:10.2514/1.20190

[10] Borglund, D., "Upper-Bound Flutter Speed Estimation Using the μ-k Method," *Journal of Aircraft*, Vol. 42, No. 2, 2005, pp. 555–557. doi:10.2514/1.7586

[11] Borglund, D., "Robust Eigenvalue Analysis Using the Structured Singular Value: The μ-p Flutter Method," *AIAA Journal*, Vol. 46, No. 11, 2008, pp. 2806–2813. doi:10.2514/1.35859

[12] Carlsson, M., and Karlsson, A., "Robust Aeroelastic Analysis of the Gripen Fighter Including Flight Test Model Validation," CEAS/AIAA/KTH International Forum on Aeroelasticity and Structural Dynamics, Paper IF-019, Stockholm, Sweden, 2007.

[13] Bäck, P., and Ringertz, U. T., "Convergence of Methods for Nonlinear Eigenvalue Problems," *AIAA Journal*, Vol. 35, No. 6, 1997, pp. 1084–1087. doi:10.2514/2.200

[14] Chen, P. C., "Damping Perturbation Method for Flutter Solution: The g-Method," *AIAA Journal*, Vol. 38, No. 9, 2000, pp. 1519–1524.

doi:10.2514/2.1171

[15] Heinze, S., "Assessment of Critical Fuel Configurations Using Robust Flutter Analysis," *Journal of Aircraft*, Vol. 44, No. 6, 2007, pp. 2034–2039.
doi:10.2514/1.30500

[16] Borglund, D., and Ringertz, U., "Solution of the Uncertain Flutter Eigenvalue Problem Using the μ-p Method," CEAS/AIAA International Forum on Aeroelasticity and Structural Dynamics, IFASD Paper 2009-048, Seattle, WA, 2009.

[17] Stark, V. J., "The AEREL Flutter Prediction System," International Council of the Aeronautical Sciences Paper 90-1.2.3, Bonn, Germany, 1990.

[18] Kouzmin, V., Kouzmin, S., Mosounov, V., and Ishmuratov, F., "Influence of Nonplanar Supersonic Interference on Aeroelastic Characteristics," *CEAS/AIAA/ICASE/NASA Langley International Forum on Aeroelasticity and Structural Dynamics*, Williamsburg, VA, NASA CP 1999-209136/PT1, 1999, pp. 415–424.

[19] Heinze, S., Ringertz, U., and Borglund, D., "Assessment of Uncertain External Store Aerodynamics Using μ-p Flutter Analysis," *Journal of Aircraft*, Vol. 46, No. 3, 2009, pp. 1062–1067.
doi:10.2514/1.39158

[20] Olert, L., and Karlsson, T., "Flutter Testing Methods at Saab Military Aircraft," *7th European Chapter Symposium*, Amsterdam, Soc. of Flight Test Engineers Paper A1994-12, Lancaster, CA, 1994.

[21] Van Overschee, P., and De Moor, B., *Subspace Identification for Linear Systems*, Kluwer Academic, Norwell, MA, 1996, pp. 90, 131.